SPACE-CLASS RUBIDIUM ATOMIC FREQUENCY STANDARD WITH IMPROVED PERFORMANCE FOR GNSS SYSTEMS

T. McClelland (*tomm@freqelec.com*), I. Pascaru, I. Shtaermann, C. Varuolo, C. Szekeley, J. Zacharski, and O. Bravo
Frequency Electronics, Inc.
55 Charles Lindbergh Boulevard, Mitchel Field, NY 11553
516-794-4500 x2104(voice), 516-794-4340 (fax)

J. White and D. Wilson
U.S. Naval Research Laboratory
4555 Overlook Avenue, SW, Washington, DC 20375, USA

Abstract

Global navigation satellite constellations such as the European Galileo, Russian GLONASS, and the USA Global Positioning Systems (GPS) employ atomic frequency standards for precision time-keeping and stable frequency generation. In addition, military jam-resistant communications satellite programs such as Milstar and its follow-on Advanced Extremely High Frequency (AEHF) are fitted with atomic standards that function as master oscillators for all frequency and timing derivation. Frequency Electronics, Inc. has developed a rubidium atomic frequency standard (RAFS) over the last 5 years for use in the most demanding satellite applications. A primary goal of this effort is a Rb standard capable of frequency stability noise floor (Allan deviation) of $\sigma_y(\tau) < 2 \times 10^{-14}$ for averaging times of up to 2,000,000 seconds (~3 weeks). The design of this RAFS unit is discussed. A summary of performance results achieved to date is also provided, including the results of a 5 month test on one RAFS unit, in vacuum, at the U.S. Naval Research Laboratory.

I. INTRODUCTION

Since 2005, Frequency Electronics, Inc. (FEI) has been working to develop a rubidium atomic frequency standard (RAFS) for the most demanding space applications, in particular the global navigation satellite systems (GNSS). This effort has leveraged FEI's experience providing Rb standards for the Milstar and AEHF satellite programs, but with a somewhat different focus. The emphasis with these earlier satellite systems was to provide a replacement for quartz oscillators which would be more immune to radiation **[1-3]**. Hence, small size, low power, and ground based tuning capability were considered more important than achieving the ultimate performance from the Rb atomic system. The goal of this current development, on the other hand, is to provide the best possible frequency and time stability from a passive rubidium atomic frequency standard capable of operating in space for at least 20 years.

This results in a different design emphasis. From a physics point of view, the architecture of the current design is very similar to the existing FEI Rb oscillator designs, based on classical optical pumping and magnetic resonance detection. This approach utilizes conventional Rb resonance lamp, filter cell and resonance cell elements, and Rb hyperfine magnetic resonance detection using transmitted resonance light. However, in order to achieve the best possible performance, temperature control of the physics

elements, improved magnetic shielding, and generation of a clean microwave excitation signal with excellent amplitude stability become the primary design drivers.
As of this writing, 1 prototype (SN 00) and 3 engineering model (SN 01, 02, and 03) RAFS units have been built and are currently in various stages of test. In this paper, a detailed description of the design of these units is provided, as well as a summary of the measured performance to date.

II. RAFS DESIGN

A photograph of one of the RAFS engineering model units is shown in Figure 1. The dimensions of the RAFS unit pictured are (L x W x H): 15 (381) x 4.6 (117) x 5.2 (132) in. (mm). This unit weighs 16.5 Lbs (7.5 kg). The unit is designed to be mounted to a baseplate using 8 mounting flanges located along each long side of the device. All electrical connections to the unit are on the top, one for power input, one for telemetry outputs, and one RF output (10 MHz).

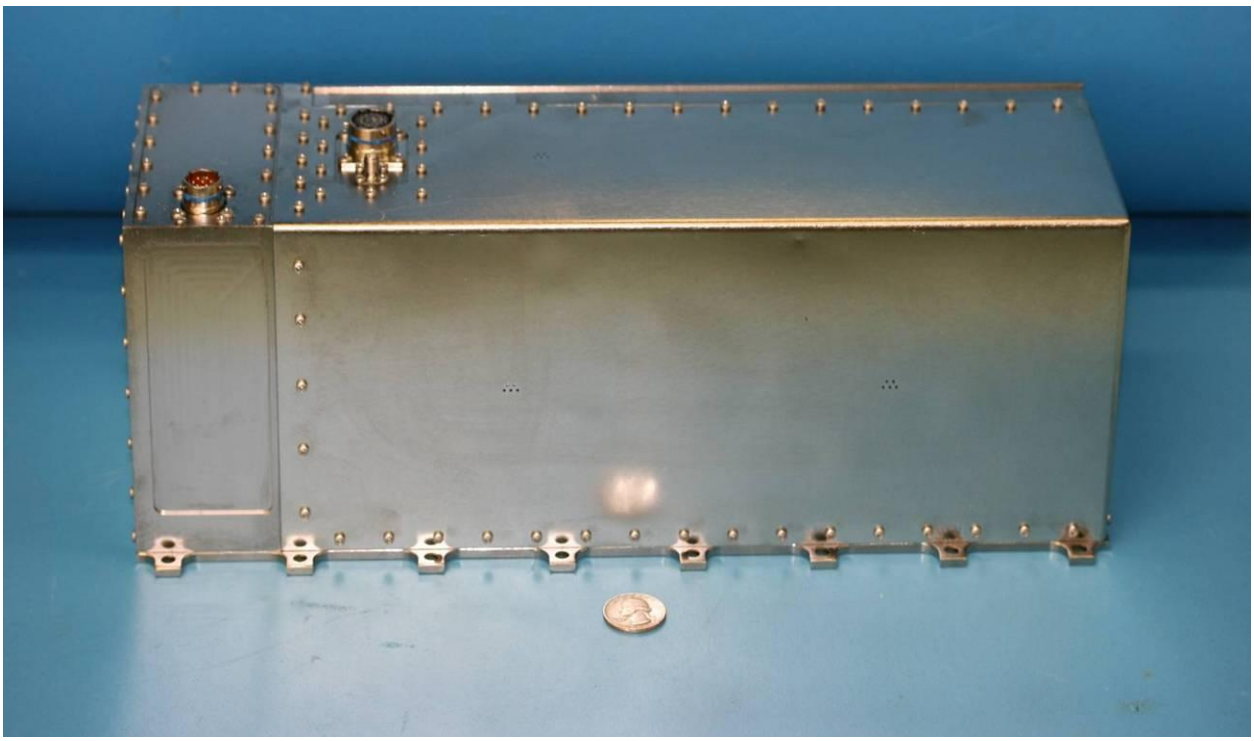

Figure 1. FEI's Next-Generation Rubidium Atomic Frequency Standard.

A block diagram of the RAFS unit is shown in Figure 2. Several key features are worthy of note. First, since frequency variation due to ambient temperature changes is typically the largest error source in Rb frequency standards, the entire system, except for the power supply, is mounted within a temperature controlled chassis. The chassis is thermally isolated from the RAFS baseplate by an insulator, with the chassis, insulator, and baseplate integrated into one RAFS assembly. The chassis temperature is maintained within ± 1°C over a mounting surface temperature range of -34 °C to + 25 °C in vacuum. The RAFS performance is optimum within this ambient temperature range; however, the RAFS unit operates up to 71 °C with somewhat diminished performance.

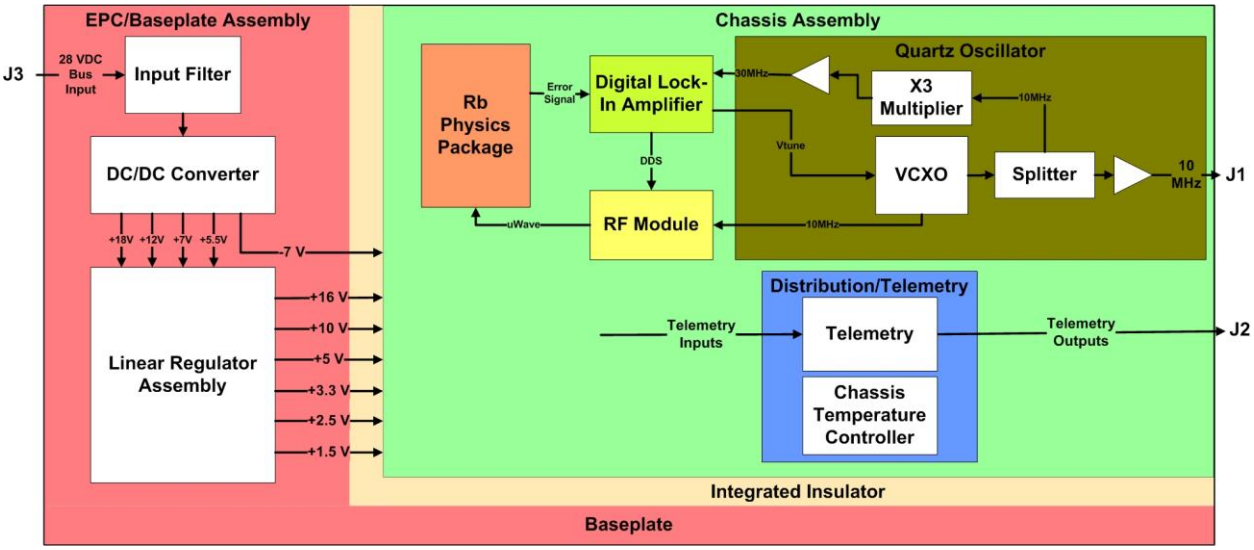

Figure 2. Overall Block diagram of RAFS unit.

A second key feature of the RAFS is its modularity. The physics package, quartz oscillator, RF module, and digital lock-in amplifier are designed, built and tested as separate, connectorized modules. This allows for an easy upgrade path to accommodate design changes necessitated by obsolete parts or to incorporate future design improvements.

DIGITAL RB CONTROL LOOP

A third key feature of the RAFS is the architecture of the Rb control loop which locks the quartz oscillator output to the Rb hyperfine resonance frequency. A block diagram of this circuitry is shown in Figure 3. The analog error signal generated in the physics package (from comparison of the microwave frequency derived from the quartz oscillator to the Rb resonance frequency) is digitized, synchronously detected, further processed digitally, then converted back to an analog voltage in order to steer the voltage controlled quartz oscillator. The digital signal processing and control functions are all implemented within a space qualified FPGA. The digital signal processing eliminates many error sources which plague Rb standards using analog control circuits such as integrator capacitor leakage, and operational amplifier input offset voltage.

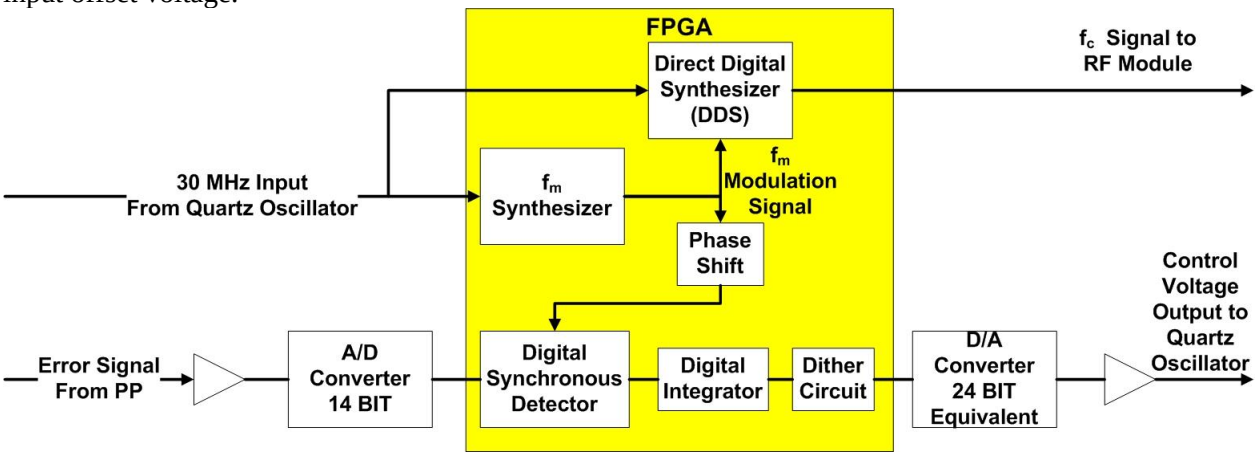

Figure 3. Block diagram of digital lock-in amplifier portion of RAFS unit.

The FPGA also includes a direct digital synthesizer (DDS) which generates the f_c signal. This signal is used in the RF module (described below) as part of the synthesis chain to generate the 6.8 GHz interrogation signal. The output of the DDS at f_c is the square-wave frequency modulated at an audio frequency, f_m , and this modulation ultimately appears on the 6.8 GHz microwave signal, and is also the frequency at which the error signal from the physics package is synchronously detected.

DIGITAL FREQUENCY TUNING WITH 1 X 10^{-14} RESOLUTION

A fourth key feature of the RAFS design is the ability to digitally tune the 10 MHz output frequency of the RAFS unit by adjusting the frequency of the DDS. As currently implemented this provides capability of frequency adjustment with ~1 x 10^{-14} resolution. A powerful advantage of this fundamental design, however, is that this adjustment resolution can be modified up or down simply by programming the FPGA with a modified DDS; no other hardware modifications are required.

The current implementation of the FPGA hard codes the frequency control word which determines the f_c frequency using resistors connected to pins of the device package. This approach does not allow further frequency tuning on orbit, but has the advantage of making the frequency control word immune from inadvertent changes (which would appear as RAFS frequency steps) due to radiation induced single event upset. Although not implemented in the RAFS units tested to date, the FPGA has space to accommodate a communications interface such as I^2C, RS-422 or MIL-STD-1553, which would allow RAFS frequency tuning using externally generated commands.

SYNTHESIS OF RB MICROWAVE RESONANCE FREQUENCY

A fifth key feature of the RAFS is the design of the frequency synthesis circuitry which generates the microwave signal at ~6.8 GHz (used to interrogate the Rb hyperfine resonance transition) from the 10 MHz quartz oscillator frequency. In order to provide the best possible RAFS frequency stability, it is crucial that the microwave signal which interrogates the Rb atoms be as "clean" as possible; that is, free of unwanted sidebands and spurious signals which can cause Bloch-Siegert frequency shifts. In addition, it is very important that the microwave signal amplitude and phase noise are small enough that the RAFS frequency stability is not impaired. With proper design, the phase noise of the microwave signal is usually not a problem; however, the amplitude stability of this signal is extremely important. Typically, the sensitivity to microwave power fluctuations is < 1 x 10^{-11}/dB.

A block diagram of the RF module which generates the 6.8 GHz signal is shown in Figure 4. Since the local oscillator (ceramic resonant oscillator – CRO) output is at only 1/3 of the desired 6.8 GHz frequency, the spectrum at 6.8 GHz after multiplication contains no sidebands within a ±2.278 GHz window. The CRO is phase locked to the quartz oscillator 10 MHz signal, and thus reproduces the quartz oscillator frequency variations within the PLL bandwidth.

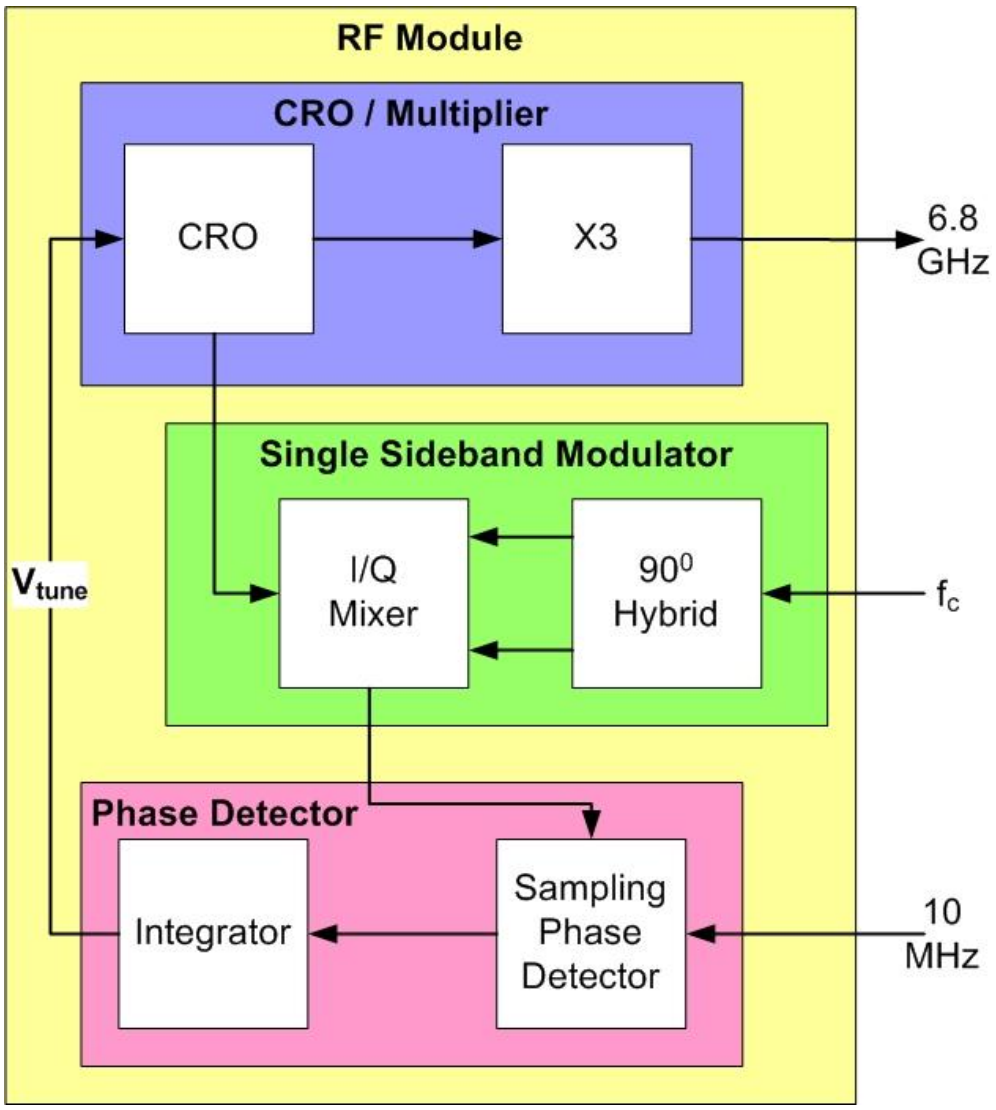

Figure 4. Block diagram of RF module portion of RAFS unit.

RADIATION HARDENED DESIGN

Special attention has been paid to radiation hardening in developing the RAFS. Although Rb atoms are inherently radiation insensitive, the electronics used to detect the Rb signal and steer a quartz oscillator must be carefully chosen in order to realize this inherent robustness in the space environment. The RAFS has been designed to meet the most stringent performance objectives even in the presence of the natural radiation environment. In order to meet this objective, several key features are critical:

1. Careful selection of electronic components which have demonstrated performance in defined radiation environments. For example, the FPGA is fuse programmed (write once), and each logic gate output results from the majority vote from 3 redundant gates receiving the same input. This voting approach provides immunity from Single Event Upset (SEU).
2. Radiation shielding, using chassis and module cover materials with adequate radiation shielding capability.
3. Spot shielding of particularly sensitive elements as necessary.

III. RAFS PERFORMANCE

The RAFS units have been tested in air, and in vacuum over an extended temperature range from -35°C to +71°C. Performance has also been measured continuously in vacuum at constant temperature for extended time periods (up to 3 months). Highlights of the measured data are presented in this section.

FREQUENCY STABILITY

Figures 5 and 6 show frequency stability data measured in vacuum. All measurements are made at FEI by comparing the RAFS units to one of three passive hydrogen masers used as frequency references. The measurements are made while the units are maintained at a constant vacuum chamber mounting plate temperature of 8°C.

Figure 5 shows summary Allan deviation information on three of the tested RAFS units. Figure 6 shows more detailed frequency stability data for SN 00 over an 80 day period of time.

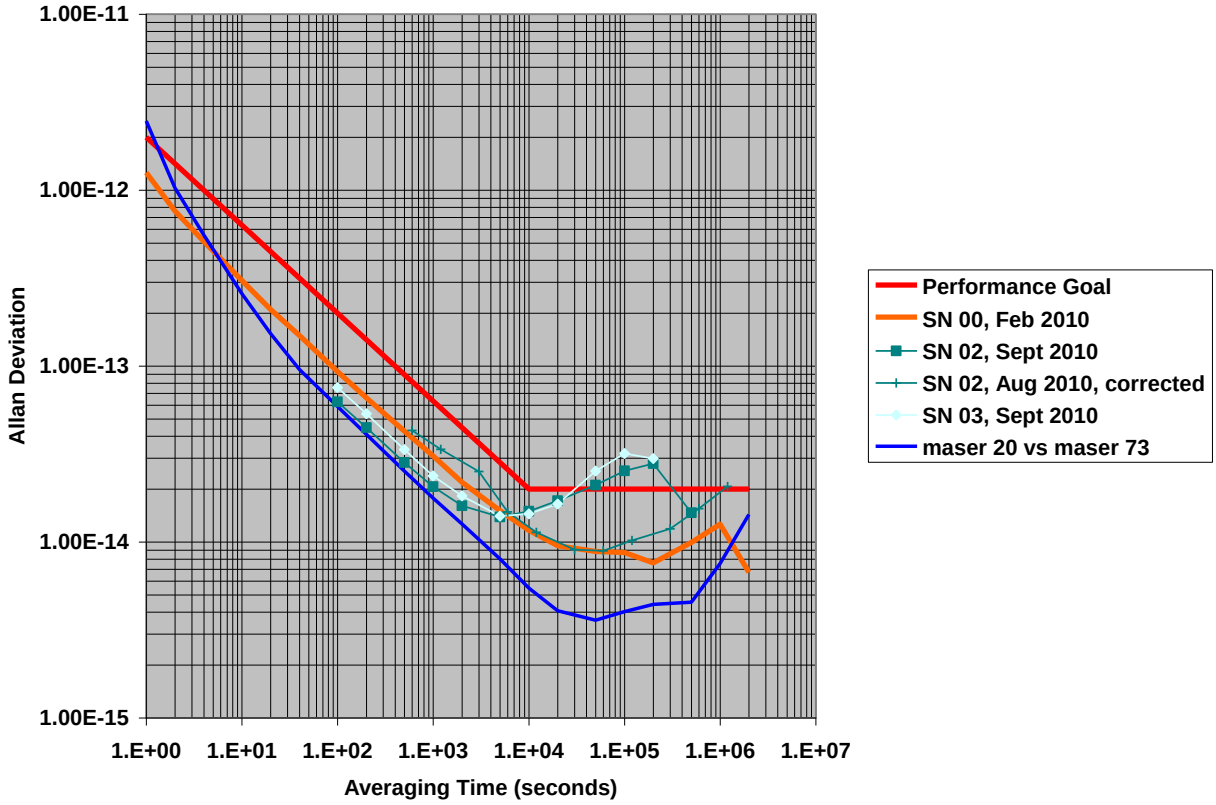

Figure 5. Frequency stability comparison of RAFS prototype units.

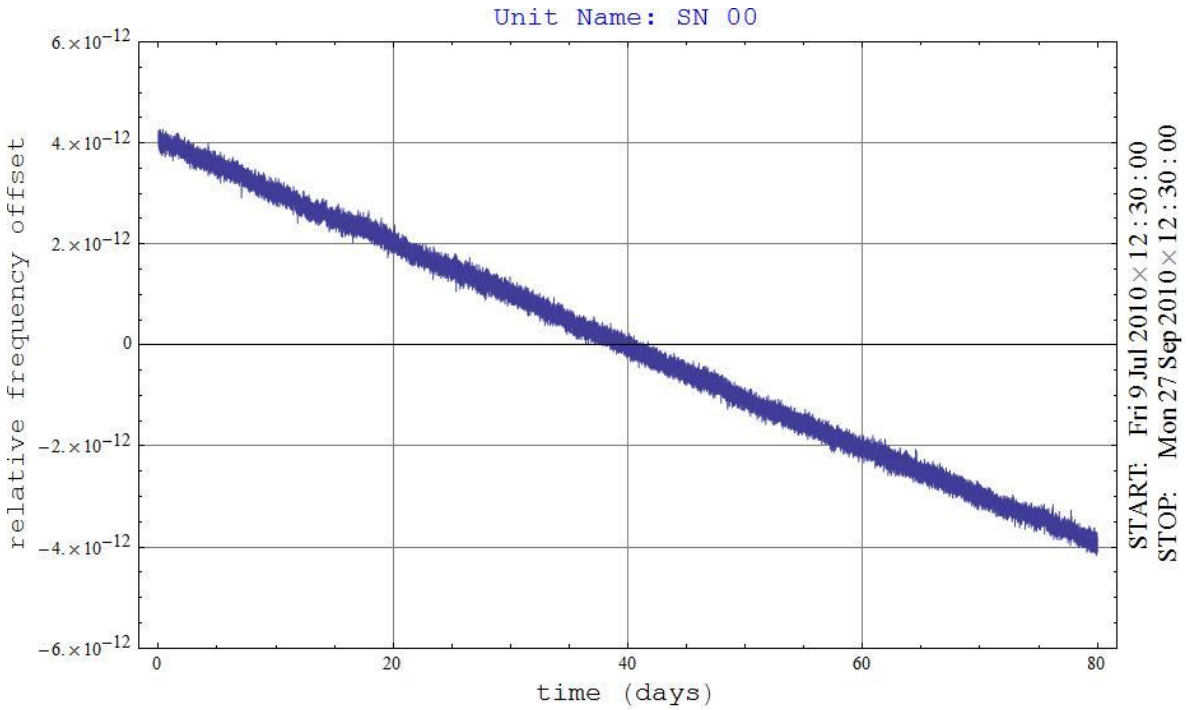

Figure 6a. Relative frequency offset of SN 00 over an 80-day period of time.

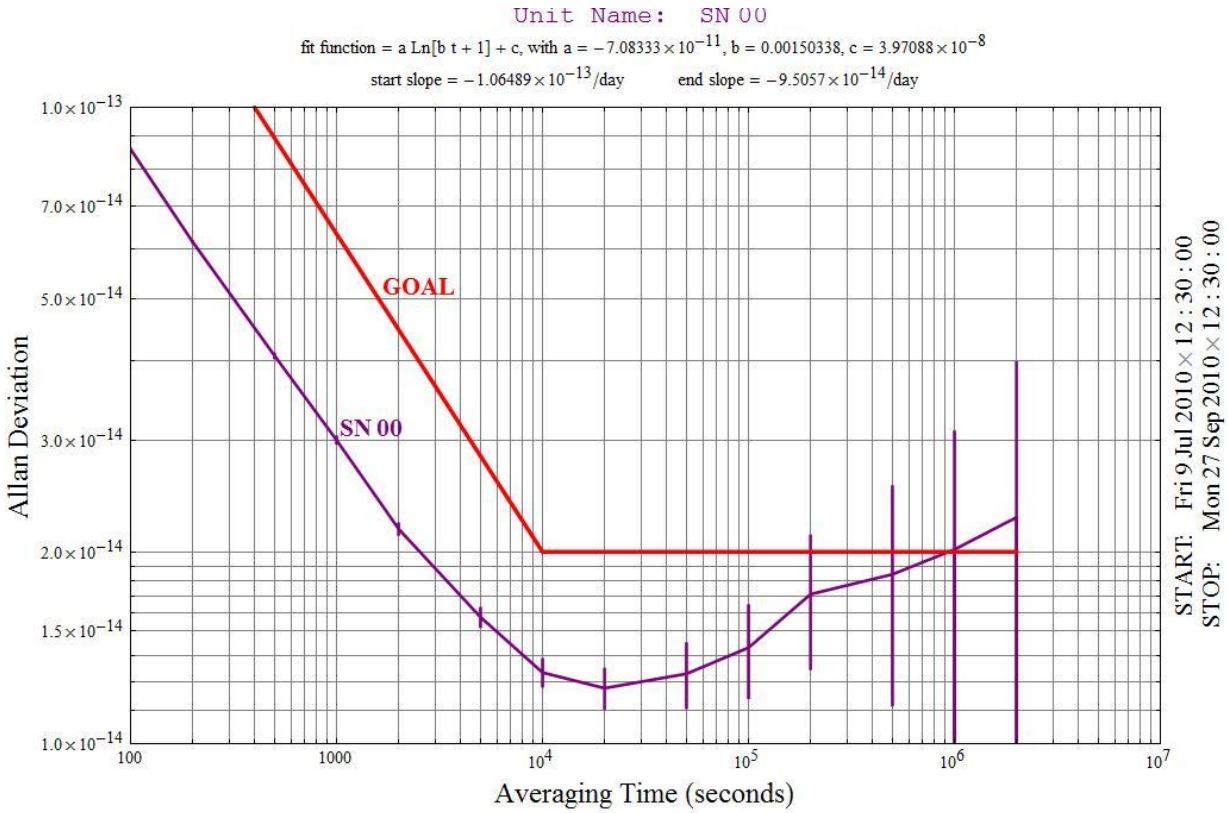

Figure 6b. Frequency stability, SN 00, calculated from the data in Figure 6a, after removal of frequency drift using a logarithmic frequency aging function.

WARM-UP TIME

A warm-up test was performed on SN 01, in vacuum. The test was performed after the unit had been powered OFF for 4 hours at a mounting plate temperature of -4°C. Both DC input power and frequency were monitored as a function of time after power-on. Input voltage was 28 VDC for this test. Figure 7 shows the results.

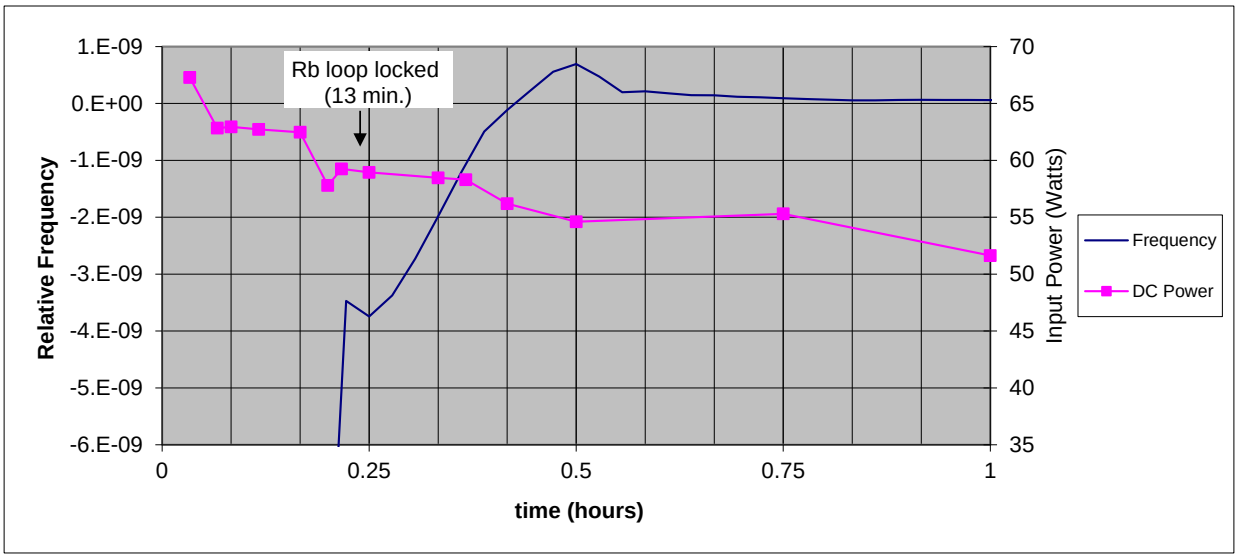

Figure 7a. Performance of RAFS SN 01 during the first hour after turn-on at -4°C. Rb control loop lock occurs at 13 minutes after turn-on.

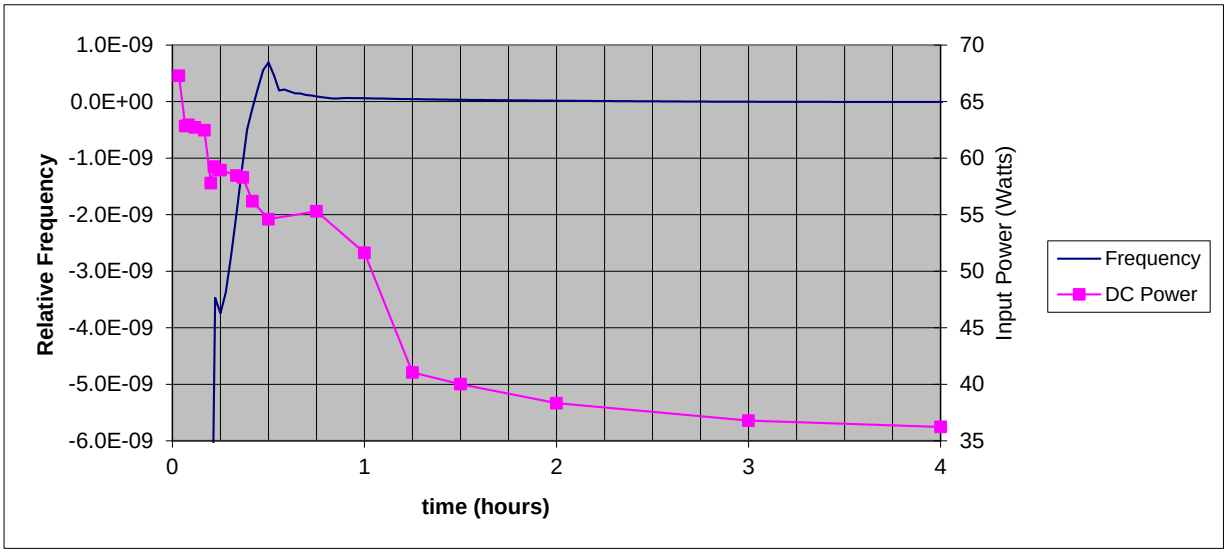

Figure 7b. Performance of RAFS SN 01 during the first 4 hours after turn-on at -4°C. DC Input power stabilizes at ~36 Watts.

PERFORMANCE OVER TEMPERATURE

SN 01 has also been tested over an extended temperature range in vacuum. The results of this test are shown in Figures 8 and 9. The RAFS is designed to operate with best performance between -35 °C and +25 °C, however, it is designed to survive and provide a continuous 10 MHz output over the extended temperature range of -35 °C to +71°C. This makes it possible for the RAFS unit to under-go qualification testing over the extended temperature range, as required on many space programs, in order to demonstrate design margin and circuit robustness.

Table 1 shows the DC input power dissipation of SN 01 at discrete mounting surface temperatures, measured during the extended temperature test in vacuum.

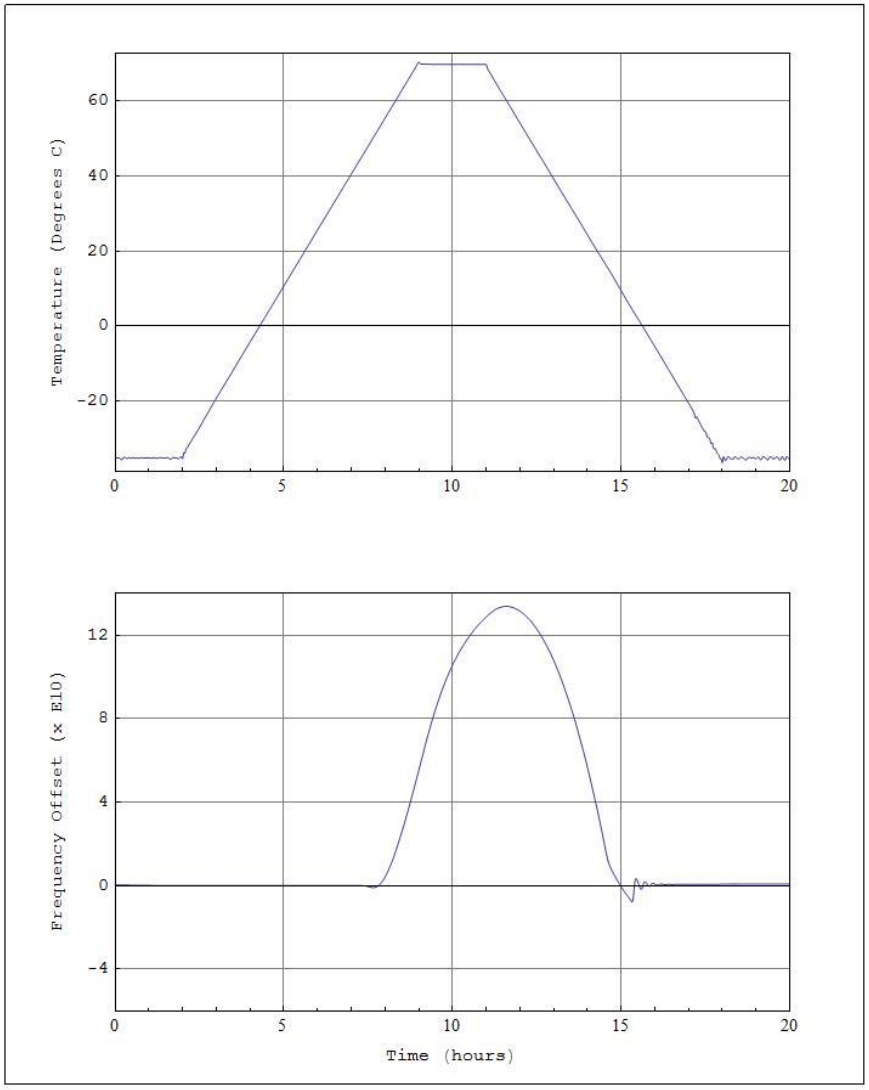

Figure 8. Frequency vs Temperature test performed on SN 01. The top plot shows the temperature profile of the vacuum system mounting plate. The bottom plot shows the corresponding frequency of the RAFS unit. Although the frequency excursion is large for temperatures above 40 °C, the unit returns to its original frequency (after a time lag) once the mounting plate temperature is reduced back to within the control range.

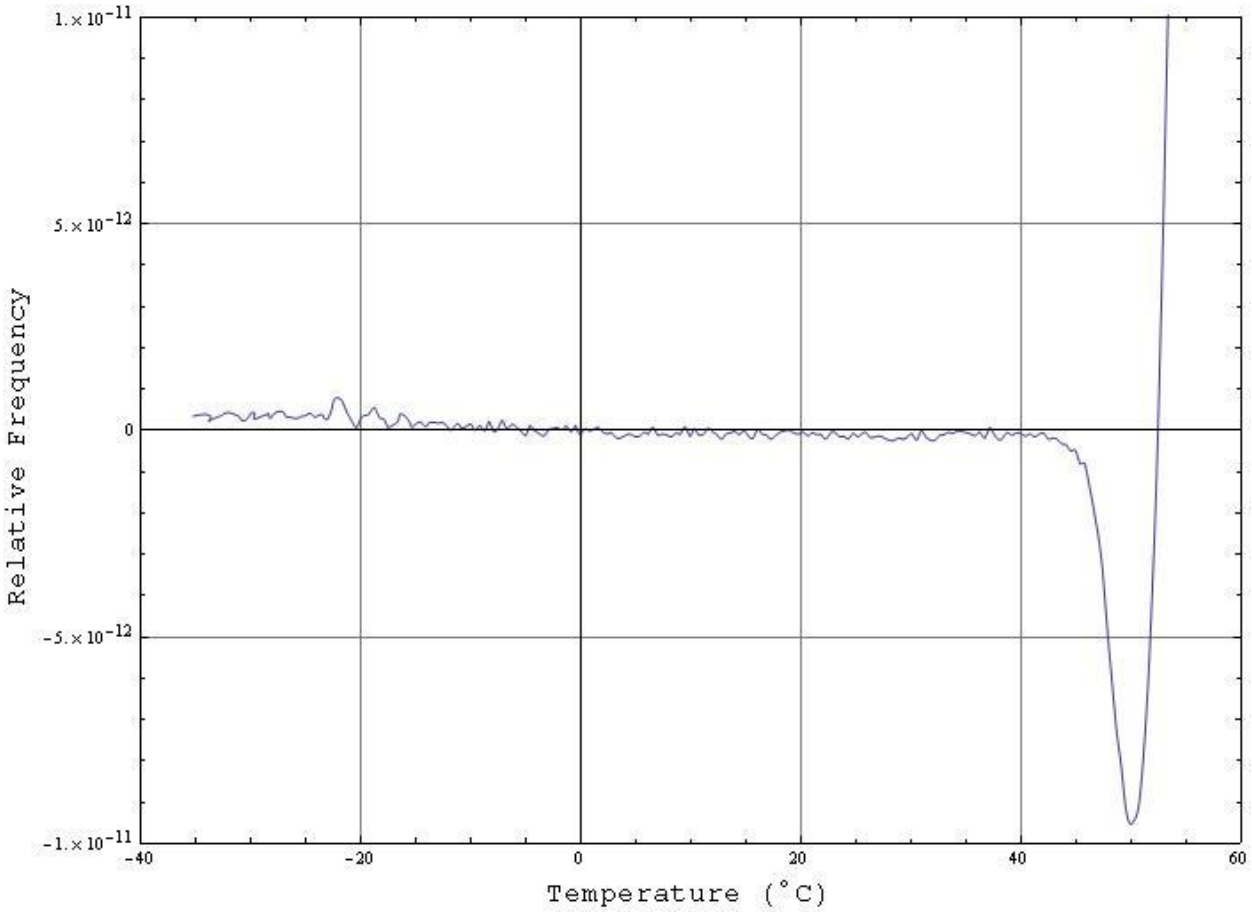

Figure 9. Frequency vs Temperature plot derived from the upward temperature ramp data shown in Figure 8. This plot shows that the frequency of the RAFS unit is stable within < 1 x 10^{-12} from -35 to +40 °C.

Table 1. Input power consumption as a function of mounting surface temperature in vacuum

SN 01 Power Consumption (Vacuum)	
Base-plate Temp (˚C)	Power Consumption (W)
71	19.91
61	20.52
9	30.85
5	31.61
-4	36.06
-5	37
-20	42.62
-24	44.41
-34	48.22

FREQUENCY VS MAGNETIC FIELD

SN 01 has also been subjected to external DC magnetic fields in order to measure the sensitivity of the RAFS to these fields. Tests were performed in a laboratory environment at room temperature by placing the RAFS unit in a Helmholtz coil. A separate test was performed with the coil magnetic field oriented along each of the primary axes of the RAFS package. Typically Rb oscillators exhibit much greater sensitivity to magnetic fields applied along the optical axis of the physics package than to fields applied perpendicular to the optical axis. This expectation was confirmed with the SN 01 tests, the sensitivity to magnetic fields along the optical axis (*x*–axis) being approximately an order of magnitude larger than the sensitivity to fields applied perpendicular (*y*, *z*-axes) to the optical axis.

Even along the optical axis, the RAFS sensitivity to magnetic fields is quite small. Therefore, the tests were performed as follows, while continuously measuring the frequency of the unit:

1. Frequency measured at 0 gauss for 30 minutes
2. Magnetic field adjusted to +3 gauss for 30 minutes
3. Magnetic field returned to 0 gauss for 30 minutes
4. Magnetic field adjusted to -3 gauss for 30 minutes
5. Magnetic field returned to 0 gauss for 30 minutes.

The results are shown graphically in Figure 10, and in tabular form in Table 2, for the test performed along the optical axis. Although not shown, the tests performed along the other two axes were performed in exactly the same way. Because the linear drift of the RAFS unit during the test was significant, calculations were made relative to a best fit linear approximation to the frequency over the entire 2.5 hour test period.

Analyzed in this way, the worst case sensitivity to magnetic fields for the RAFS unit is $< 1 \times 10^{-13}$/gauss, for magnetic fields applied in any direction of up to 3 gauss.

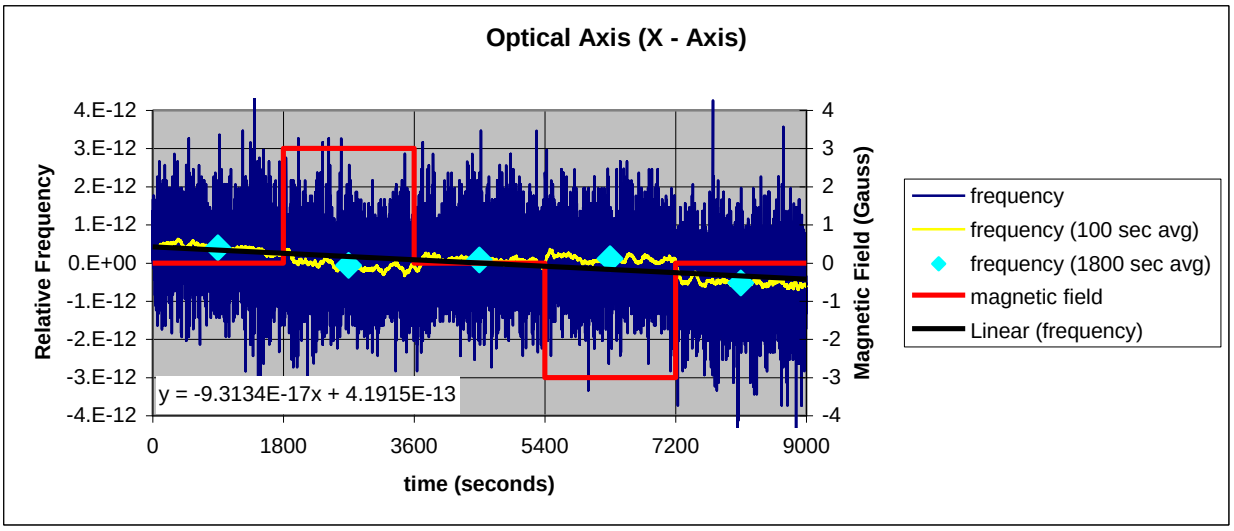

Figure 10. Magnetic field sensitivity test results for magnetic field applied along the optical axis. Frequency measurements (one second averages) are shown in blue. A 100 second moving average is shown in yellow, and a single average frequency computed for each magnetic field setting interval is shown in light blue. The magnetic field setting is shown in red.

Table 2. Computations based on the data shown in Figure 10.

Optical Axis (X - Axis)		
magnetic field (gauss)	Δ (freq - fit line)	df/dH (1/gauss)
3	-2.27E-13	-7.6E-14
-3	2.79E-13	-9.3E-14
	mean sensitivity:	**-8.4E-14/Gauss**

TESTS PERFORMED AT NRL

The SN 03 unit was tested continuously, at constant temperature (8°C) in vacuum at the Naval Research Laboratory (NRL) from September 18, 2010 to February 14, 2011 (151 days). A plot of the relative frequency offset during this test is shown in Figure 11. The performance of this unit during the test at NRL is very similar to the previously observed performance at FEI. However, two abrupt frequency excursions were observed during the test at NRL. The first was on November 21, 2010 (the 64th day of the test) of magnitude ~4 x 10^{-13}, and the second was on February 8, 2011 (the 143rd day of the test) of magnitude ~7 x 10^{-13}. These frequency steps coincide, in each case, with an abrupt change in the DC light transmitted through the physics package. Although correlation is not necessarily causation, the data are consistent with a sensitivity to transmitted light of 5.3 x 10^{-13}/milli-volt. The root cause of these excursions is currently under investigation; however, a preliminary assessment is that they are caused by movement of Rb metal in one of the cells in the physics package. Design modifications to minimize this effect have been implemented.

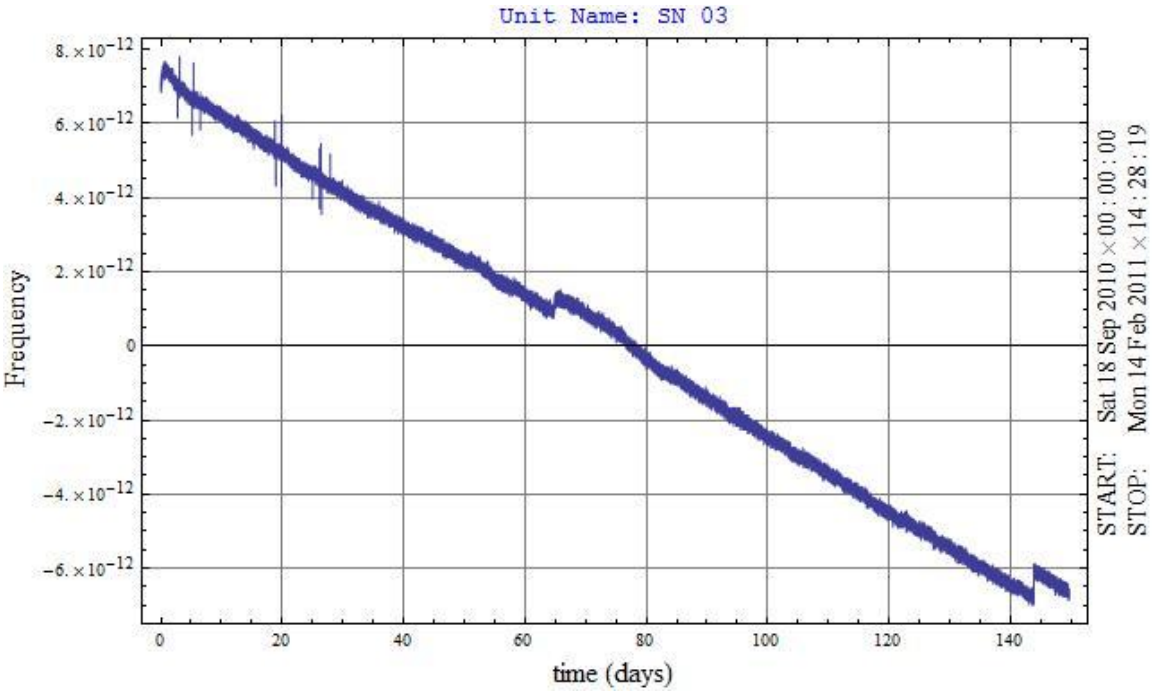

Figure 11. Relative frequency offset of SN 03 during test at constant temperature in vacuum at the Naval Research Laboratory (NRL). The frequency drift was approximately linear during this test, with magnitude ~ -1 x 10^{-13}/day. Two frequency steps occurred, the first on November 21, 2010, and the second on February 8, 2011.

The performance of the SN 03 unit at NRL, for ~60 days prior to the first frequency step, as well as the performance for ~60 days after this step, are similar to performance measured at FEI. Allan deviation frequency stability results for these time periods are shown in Figures 12 and 13. A plot comparing the Allan deviation results from Figure 12, Figure 13, and the result when all the data are used is shown in Figure 14.

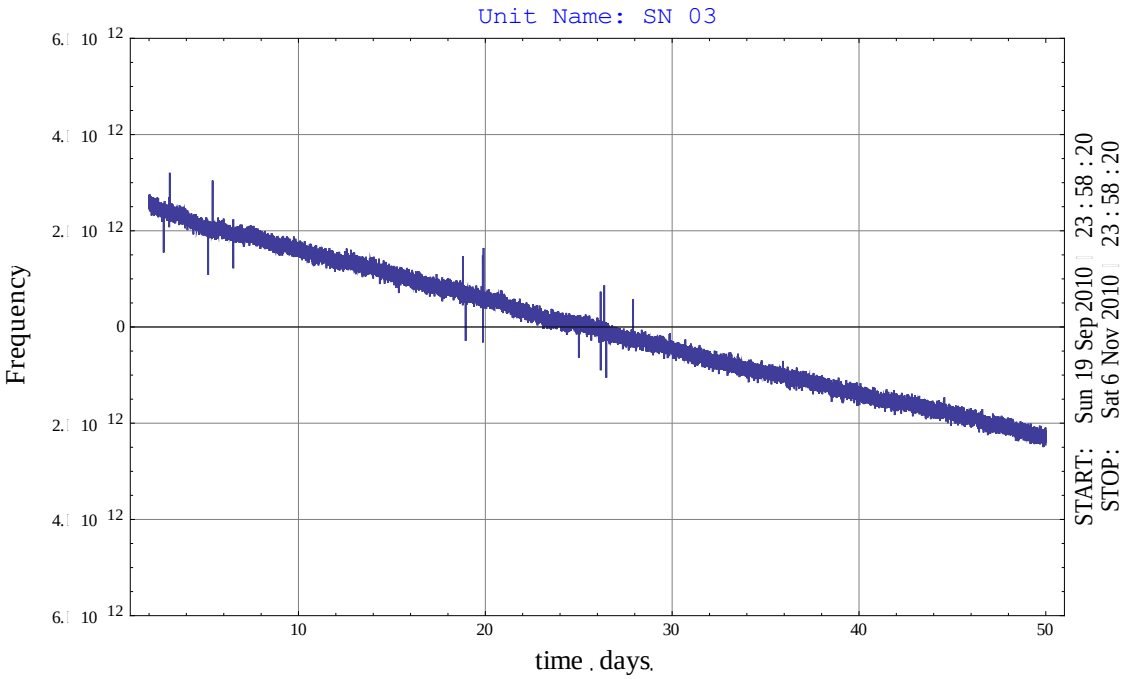

Figure 12a. Relative frequency offset of SN 03 from September 19 to November 6, 2010.

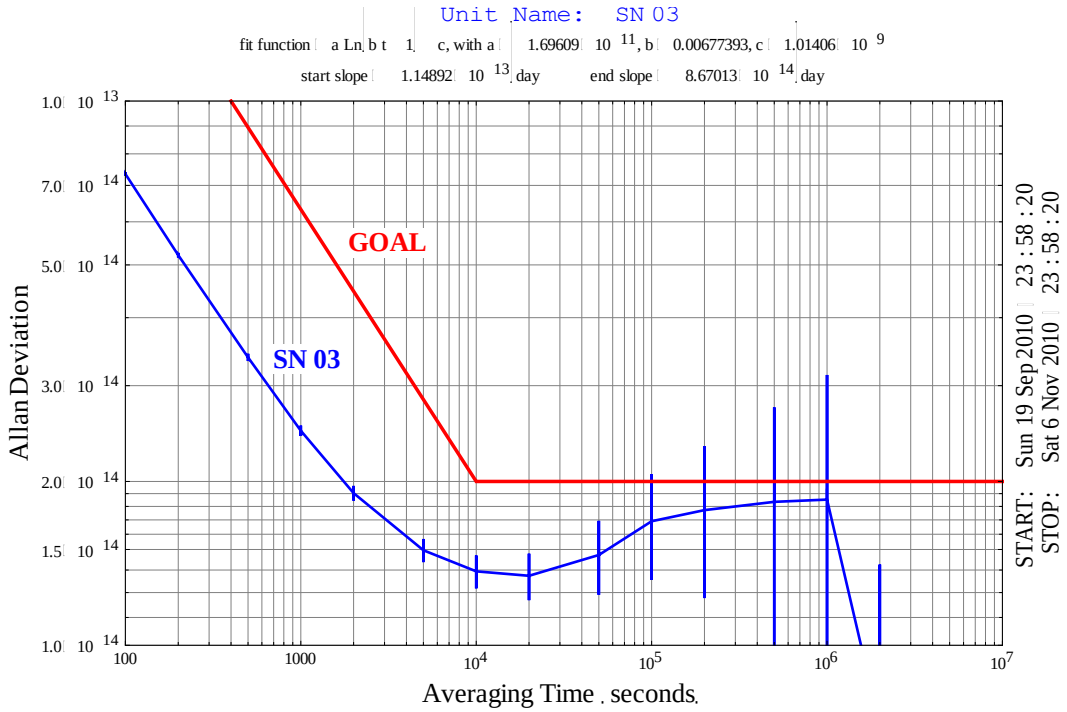

Figure 12b. Frequency stability, SN 03, calculated from the data in Figure 12a, after removal of frequency drift using a logarithmic frequency aging function.

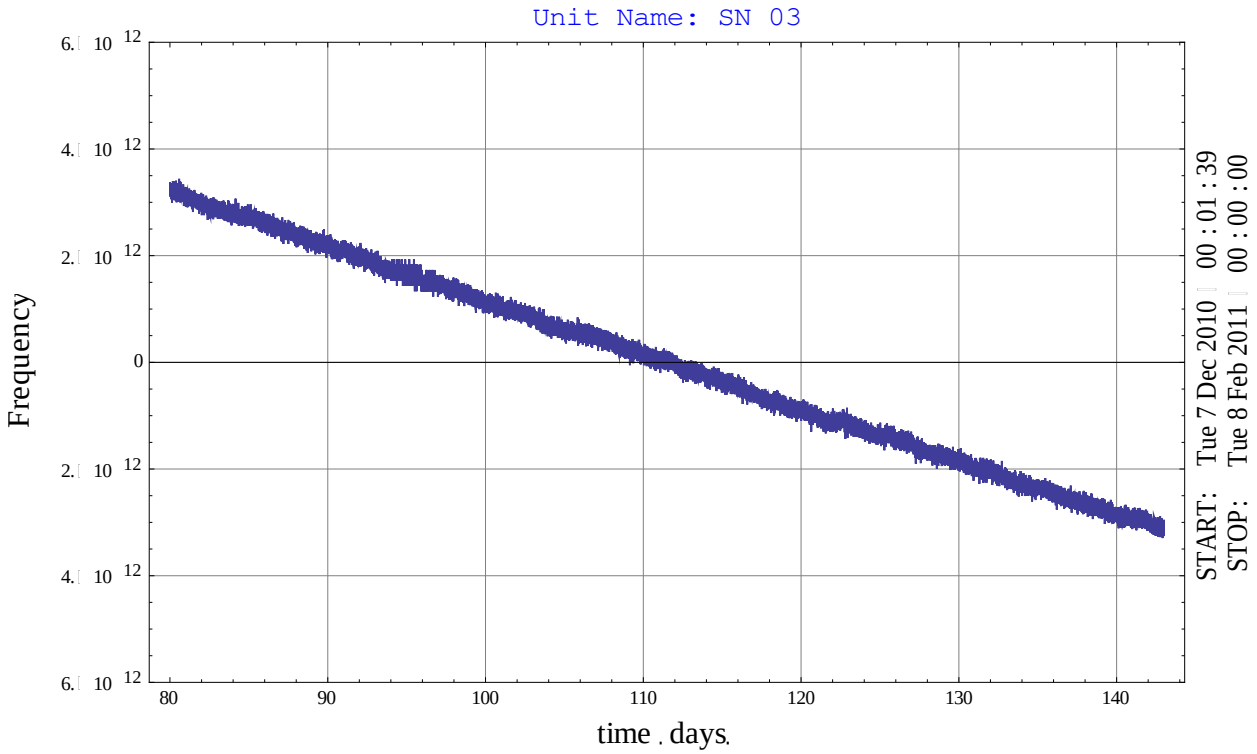

Figure 13a. Relative frequency offset of SN 03 from Dec. 7, 2010 to Feb. 8, 2011.

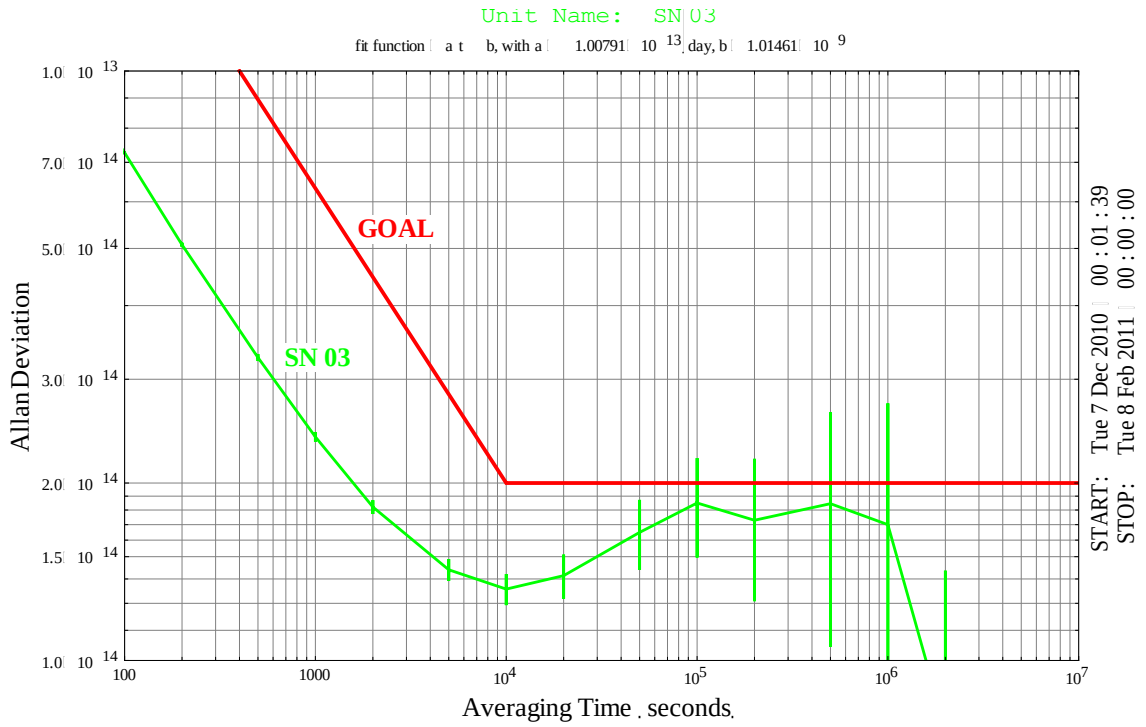

Figure 13b. Frequency stability, SN 03, calculated from the data in Figure 13a, after removal of frequency drift using a linear frequency aging function.

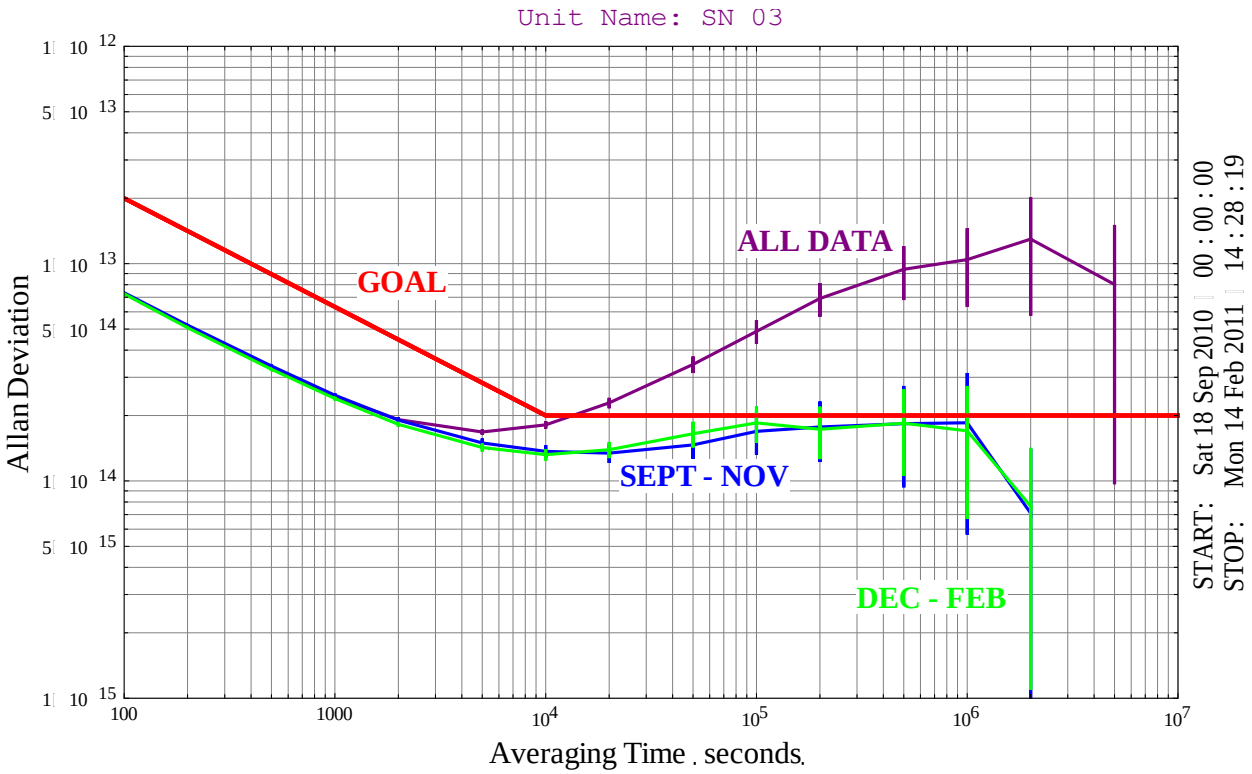

Figure 14. Frequency stability of the SN 03 unit during the test at NRL. The purple line is the Allan deviation calculated using all the data, including the two frequency steps shown in Figure 11. The blue line is the Allan deviation calculated from ~50 days between September and November, and the green line is the Allan deviation calculated from ~60 days between December and February.

IV. SUMMARY

FEI has developed a RAFS unit for the most demanding GNSS satellite applications. The unit incorporates a modular design approach, and digital control loop architecture implemented in a space qualified, radiation hardened FPGA. This approach provides for easy upgrades at the module level to accommodate obsolescence issues, as well as a path to performance enhancements through firmware upgrades to the FPGA that do not impact the hardware design. Although the current implementation provides a fixed frequency output at 10 MHz nominal, remote frequency tuning with resolution of 1×10^{-14} requires only the addition of communication interface software to the FPGA.

RAFS units have been tested in a variety of environments including:

- Temperature (-35°C to +71°C) in vacuum
- Warmup from OFF condition (-4°C) in vacuum
- Magnetic Field (-3 gauss to +3 gauss)
- Continuous extended operation at 8°C in vacuum.
-

Although optimized for best performance between -35°C and +40°C, the unit functions with reduced performance over the extended temperature range of -35°C to +71°C. This capability makes possible qualification and acceptance testing of flight units (conforming to a "test as you fly" philosophy) over the

extended temperature range in order to demonstrate design margin with respect to anticipated on orbit environments.

Performance over an extended period of time in vacuum has been demonstrated with frequency stability of:

$$\sigma_y(\tau) < 9 \times 10^{-13}/\sqrt{\tau} + 2 \times 10^{-14} \text{ for } \tau \text{ between 1 and 1,000,000 seconds.}$$

V. ACKNOWLEDGEMENTS

This work has been supported in part by initial funding from the USAF GPS Directorate under contract FA880705-C-0007, and subsequent funding from ITT Corporation in support of the GPS III program.

VI. REFERENCES

[1] M.B. Bloch, O. Mancini, and T. McClelland, 2002, *"Performance of Quartz and Rubidium Clocks in Space,"* in IEEE International Frequency Symposium 2002, 29-31 May 2002, New Orleans, Louisiana, pp. 505-509.

[2] N. D. Bhaskar, A. D. Matt, N. Russo, T. McClelland, M. Bloch, and M. Meirs, 1997, *"On-orbit performance of Milstar Rubidium and Quartz Frequency Standards,"* in IEEE International Frequency Symposium 1997, 28-30 May 1997, Orlando, Florida, pp. 329-337.

[3] J. C. Camparo, R. P. Frueholz, and A. P. Dubin, 1998, *"Precise Time Synchronization of Two Milstar Communications Satellites Without Ground Intervention"* **International Journal of Satellite Communications, Vol. 15**, Issue 3, 135-139.